JOURNAL OF THEORETICAL
AND APPLIED MECHANICS
https://doi.org/10.15632/jtam-pl/205104
ONLINE FIRST

ELASTIC BUCKLING OF AN INDIVIDUAL I-BEAM WITH CONSIDERATION OF THE SHEAR EFFECT

Krzysztof MAGNUCKI

Łukasiewicz Research Network, Poznan Institute of Technology, Poznan, Poland
krzysztof.magnucki@pit.lukasiewicz.gov.pl

The subject of the paper is a homogeneous I-beam with an individual shape web. The beam, simply supported at one end and at the other simply supported with elastic limitation of rotation, is subjected to axial compression by a force F. The analytical model of the beam is developed with consideration of the shear effect. The deformation of the beam's plane cross-section after buckling is determined analytically, taking into account the classical expression for shear stresses in a beam (known as Zhuravsky or Jourawski shear stress). Longitudinal displacements, strains, and stresses are then formulated. Based on the principle of stationary total potential energy, a system of two equilibrium differential equations is derived. These equations are solved analytically, taking into account the beam support conditions, and the critical force FCR is determined. Detailed calculations are realized for sample beams.

Keywords: analytical modeling; I-beam; elastic buckling; shear effect.

1. Introduction

Initiated by Leonhard Euler in the 18th century, the study of buckling of a compressed beam has been intensively developed over the following centuries and is still being improved today to address problems related to the stability of beams, plates, and shells, which are closely related to the design of structures. Rykaluk (2012) described in detail the criteria of elastic stability, buckling issues of axially and eccentrically compressed classical and thin-walled beams with open cross-sections, buckling of rings and arches, stability of flat frames, as well as stability problems of rectangular plates and shells. Magnucki and Milecki (2015) examined the elastic buckling problem of the symmetrical triangular frame under tensile in-plane load. They studied in detail both analytically and numerically (using FEM) the in-plane buckling state and the lateral buckling state of this sample frame. Simão (2017) presented a stability analysis of shear-sensitive columns with a linear formulation according to the Timoshenko beam theory along with a nonlinear shear formula. Eslami (2018) first characterized the stability concept and then presented in detail buckling and post-buckling problems of beams and plates, as well as buckling problems of cylindrical, spherical and conical shells. Yang *et al.* (2019) presented the results of multiple numerical and experimental studies of the global buckling problem of bi-symmetrical steel beams under three-point bending. Szymczak and Kujawa (2019) investigated analytically and

Ministry of Science and Higher Education
Republic of Poland

This publication has been funded by the Polish Ministry of Science and Higher Education under the Excellent Science II programme "Support for scientific conferences".
The content of this article was presented during the 61st Symposium "Modelowanie w mechanice" (Modelling in Mechanics), Szczyrk, Poland, March 2–5, 2025.

numerically (FEM) the flexural buckling of axially compressed, simply supported, and clamped I-columns made of aluminum alloy and indicated the influence of material non-linearity on the critical loads. Genovese and Elishakoff (2019) pointed out the importance of the principle of virtual work in the formulation of planar static rod theories with consideration of large deformations and the transverse shear effect. Filho *et al.* (2022) investigated, both experimentally and numerically, the buckling problem of welded I-section columns undergoing flexural or torsional buckling failure. Yang *et al.* (2023) focused on the buckling instability problem of I-beams, developed a numerical model of the beam using Lagrange polynomials to describe the three-dimensional displacement field, and numerically investigated the global buckling, local buckling, and global–local coupled buckling of these beams. Jing *et al.* (2024) studied the effect of limiting the beam center deflection with an elastic support on the critical axial force and dynamic characteristics. They determined two stable states of beam buckling depending on the stiffness of the elastic center support.

Magnucki and Sowiński (2024) applied an individual nonlinear shear deformation theory to the analytical modeling of a clamped sandwich beam with a functionally graded core, and then analytically and numerically (using FEM) studied the bending of this beam under a uniformly distributed load. Magnucki (2024a) developed two analytical models of a five-layered composite beam. The first is formulated on the basis of the classical zig-zag theory, while the second is developed using the nonlinear shear deformation theory. He then analytically studied the bending of these sample beams for both models. Magnucki (2024b) analytically described the cross-section of a standard wide-flange H-beam as a three-layer structure and analytically studied the fundamental natural frequency of these sample beams with consideration of the shear effect. Couto *et al.* (2025) provided a thorough review of the research that led to the proposal of European fire design rules for steel thin-walled I-beams. They focused on the problem of interaction between local and global buckling in these members.

This work continues studies of the beam buckling problems presented in the above sample papers. The main goal of the work is to analytically study the beam buckling with consideration of the shear effect.

2. Analytical study of the individual I-beam with consideration of the shear effect

The subject of the study is a homogeneous individual I-beam of length L, width b, and total depth h under axial compression by a force F. One end of the beam is simply supported, while the other end is elastically limited in rotation by means of a rigid part connected to two springs with stiffness k_s (Fig. 1). The beam is protected against out of the x- and y-plane buckling.

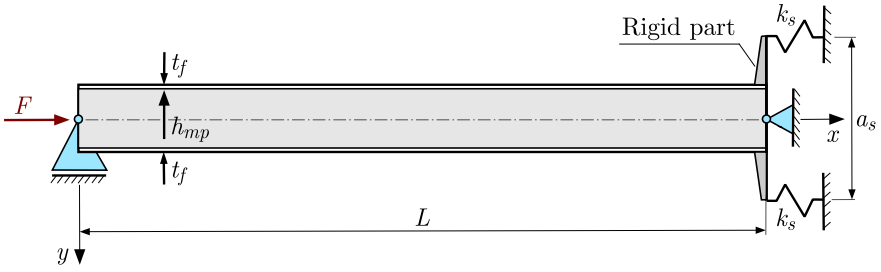

Fig. 1. Schematic diagram of the beam with two different supports at its ends.

The cross-section of this beam, with a functionally graded middle part-web thickness, is shown in Fig. 2. This individual beam's planar cross-section provides input for analytically determining the nonlinear function of its deformation.

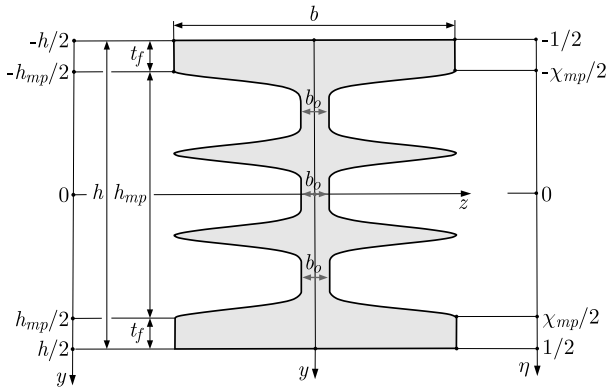

Fig. 2. Schematic cross-section of the individual beam.

The widths of the successive parts of this cross-section are as follows:

– the upper flange ($-1/2 \leq \eta \leq -\chi_{mp}/2$):

$$\overline{w}_{uf}(\eta) = \frac{w_{uf}(\eta)}{b} = 1, \tag{2.1}$$

– the middle part – web ($-\chi_{mp}/2 \leq \eta \leq \chi_{mp}/2$):

$$\overline{w}_{mp}(\eta) = \frac{w_{mp}(\eta)}{b} = \beta_0 + (1-\beta_0)\sin^n\left(3\pi\frac{\eta}{\chi_{mp}}\right), \tag{2.2}$$

– the lower flange ($\chi_{mp}/2 \leq \eta \leq 1/2$):

$$\overline{w}_{lf}(\eta) = \frac{w_{lf}(\eta)}{b} = 1, \tag{2.3}$$

where $\eta = y/h$ – dimensionless coordinate, $\chi_{mp} = h_{mp}/h$, $\beta_0 = b_0/b$ – dimensionless sizes, and n – even number.

Taking into account the papers by Magnucki (2024a) and Magnucki (2024b), the dimensionless deformation functions for the successive parts of this cross-section are analytically determined as follows:

– the upper flange ($-1/2 \leq \eta \leq -\chi_{mp}/2$):

The dimensionless first moment (Fig. 3) is given by

$$\overline{S}_z^{(uf)}(\eta) = \frac{S_z^{(uf)}(\eta)}{bh^2} = -\int_{-1/2}^{-\eta} \eta\,\mathrm{d}\eta = \frac{1}{8}(1-4\eta^2). \tag{2.4}$$

Therefore, the derivative of the dimensionless deformation function is

$$\frac{\mathrm{d}f_d^{(uf)}}{\mathrm{d}\eta} = \frac{\overline{S}_z^{(uf)}(\eta)}{\overline{w}_{uf}(\eta)} = \frac{1}{8}(1-4\eta^2). \tag{2.5}$$

Consequently, the dimensionless deformation function is

$$f_d^{(uf)}(\eta) = -C_f + \frac{1}{8}\left(1-\frac{4}{3}\eta^2\right)\eta, \tag{2.6}$$

where the integration constant:

$$C_f = -\frac{1}{16}\left(1-\frac{1}{3}\chi_{mp}^2\right)\chi_{mp} + \int_0^{\chi_{mp}/2} \frac{\overline{S}_z^{(mp)}(\eta)}{\overline{w}_{mp}(\eta)}\,\mathrm{d}\eta; \tag{2.7}$$

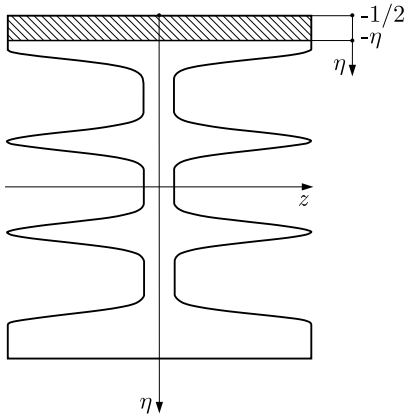

Fig. 3. Hatched area of the upper flange selected part.

– the middle part–web ($-\chi_{mp}/2 \leq \eta \leq \chi_{mp}/2$):
The dimensionless first moment (Fig. 4) is given by

$$\overline{S}_z^{(mp)}(\eta) = \frac{1}{8}\left(1-\chi_{mp}^2\right) - \int\limits_{-\chi_{mp}/2}^{\eta} \eta \overline{w}_{mp}(\eta)\,\mathrm{d}\eta. \tag{2.8}$$

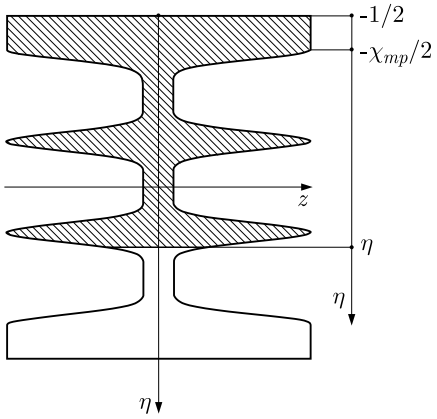

Fig. 4. Hatched area of the selected part of the functionally graded middle part-web.

The derivative of the dimensionless deformation function is

$$\frac{\mathrm{d}f_d^{(mp)}}{\mathrm{d}\eta} = \frac{\overline{S}_z^{(mp)}(\eta)}{\overline{w}_{mp}(\eta)} \tag{2.9}$$

and the dimensionless deformation function is

$$f_d^{(mp)}(\eta) = \int \frac{\overline{S}_z^{(mp)}(\eta)}{\overline{w}_{mp}(\eta)}\,\mathrm{d}\eta, \tag{2.10}$$

– the lower flange ($\chi_{mp}/2 \leq \eta \leq 1/2$):

$$\overline{S}_z^{(lf)}(\eta) = \frac{1}{8}(1-4\eta^2), \tag{2.11}$$

$$\frac{\mathrm{d}f_d^{(lf)}}{\mathrm{d}\eta} = \frac{1}{8}(1-4\eta^2), \tag{2.12}$$

$$f_d^{(lf)}(\eta) = C_f + \frac{1}{8}\left(1-\frac{4}{3}\eta^2\right)\eta. \tag{2.13}$$

The schematic cross-section of the beam, and graphs of dimensionless deformation functions of the planar cross-section (2.6), (2.10), (2.13), and its derivatives (2.5), (2.9), (2.12) for the example beam ($\chi_{mp} = 4/5$, $\beta_0 = 1/10$, $n = 10$) are shown in Fig. 5.

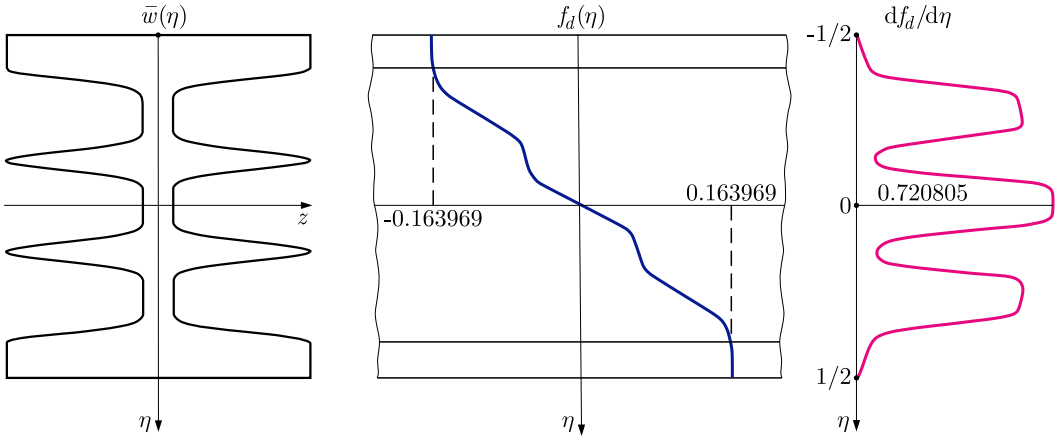

Fig. 5. Schematic cross-section of the beam and graphs of functions $f_d(\eta)$, $\mathrm{d}f_d/\mathrm{d}\eta$.

The deformation of a planar cross-section of this beam, in accordance with the nonlinear shear deformation theory, is shown in Fig. 6.

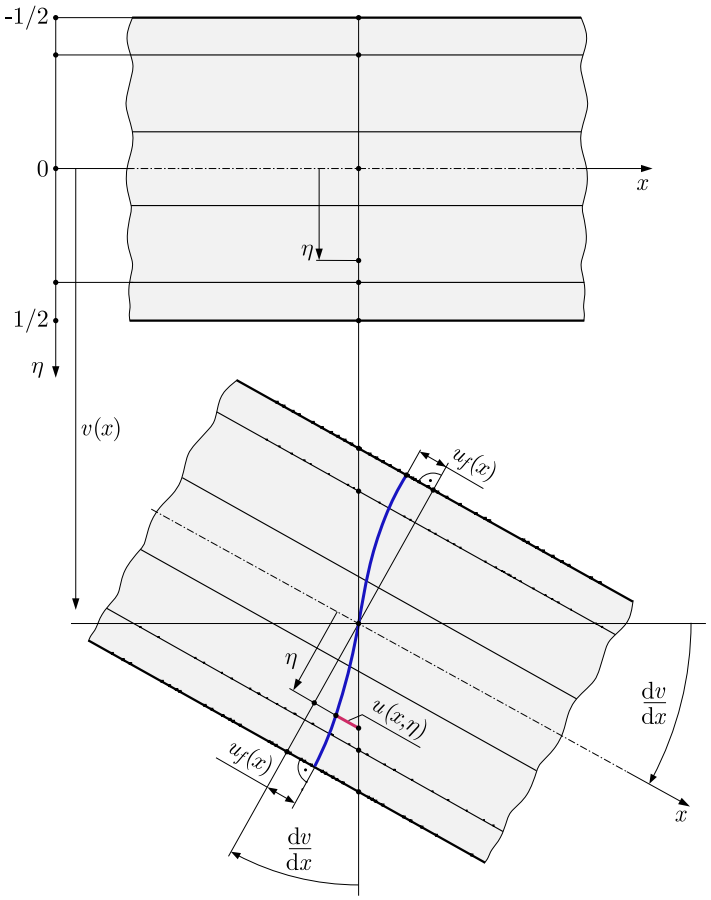

Fig. 6. Schematic diagram of planar cross-section deformation of the beam.

Based on this diagram (Fig. 6), the longitudinal displacements, and consequently strains and stresses, in the successive parts of this cross-section are as follows:

– upper flange ($-1/2 \leq \eta \leq -\chi_{mp}/2$):

$$u^{(uf)}(x,\eta) = -h\left[\eta\frac{\mathrm{d}v}{\mathrm{d}x} - f_d^{(uf)}(\eta)\psi_f(x)\right], \tag{2.14}$$

$$\varepsilon_x^{(uf)}(x,\eta) = -h\left[\eta\frac{\mathrm{d}^2v}{\mathrm{d}x^2} - f_d^{(uf)}(\eta)\frac{\mathrm{d}\psi_f}{\mathrm{d}x}\right], \tag{2.15}$$

$$\gamma_{xy}^{(uf)}(x,\eta) = \frac{\mathrm{d}f_d^{(uf)}}{\mathrm{d}\eta}\psi_f(x), \tag{2.16}$$

$$\sigma_x^{(uf)}(x,\eta) = E\,\varepsilon_x^{(uf)}(x,\eta), \tag{2.17}$$

$$\tau_{xy}^{(uf)}(x,\eta) = \frac{E}{2(1+\nu)}\gamma_{xy}^{(uf)}(x,\eta), \tag{2.18}$$

– the middle part – web ($-\chi_{mp}/2 \leq \eta \leq \chi_{mp}/2$):

$$u^{(mp)}(x,\eta) = -h\left[\eta\frac{\mathrm{d}v}{\mathrm{d}x} - f_d^{(mp)}(\eta)\psi_f(x)\right], \tag{2.19}$$

$$\varepsilon_x^{(mp)}(x,\eta) = -h\left[\eta\frac{\mathrm{d}^2v}{\mathrm{d}x^2} - f_d^{(mp)}(\eta)\frac{\mathrm{d}\psi_f}{\mathrm{d}x}\right], \tag{2.20}$$

$$\gamma_{xy}^{(mp)}(x,\eta) = \frac{\mathrm{d}f_d^{(mp)}}{\mathrm{d}\eta}\psi_f(x), \tag{2.21}$$

$$\sigma_x^{(mp)}(x,\eta) = E\,\varepsilon_x^{(mp)}(x,\eta), \tag{2.22}$$

$$\tau_{xy}^{(mp)}(x,\eta) = \frac{E}{2(1+\nu)}\gamma_{xy}^{(mp)}(x,\eta), \tag{2.23}$$

– the lower flange ($\chi_{mp}/2 \leq \eta \leq 1/2$):

$$u^{(lf)}(x,\eta) = -h\left[\eta\frac{\mathrm{d}v}{\mathrm{d}x} - f_d^{(lf)}(\eta)\psi_f(x)\right], \tag{2.24}$$

$$\varepsilon_x^{(lf)}(x,\eta) = -h\left[\eta\frac{\mathrm{d}^2v}{\mathrm{d}x^2} - f_d^{(lf)}(\eta)\frac{\mathrm{d}\psi_f}{\mathrm{d}x}\right], \tag{2.25}$$

$$\gamma_{xy}^{(lf)}(x,\eta) = \frac{\mathrm{d}f_d^{(lf)}}{\mathrm{d}\eta}\psi_f(x), \tag{2.26}$$

$$\sigma_x^{(lf)}(x,\eta) = E\,\varepsilon_x^{(lf)}(x,\eta), \tag{2.27}$$

$$\tau_{xy}^{(lf)}(x,\eta) = \frac{E}{2(1+\nu)}\gamma_{xy}^{(lf)}(x,\eta), \tag{2.28}$$

where E – Young's modulus, ν – Poisson's ratio.

Based on the principle of stationary total potential energy, after simple transformation, the system of two differential equilibrium equations for this beam is obtained in the following form:

$$\overline{J}_z \frac{\mathrm{d}^2 v}{\mathrm{d}x^2} - C_{v\psi} \frac{\mathrm{d}\psi_f}{\mathrm{d}x} = -\frac{M_b(x)}{Ebh^3}, \tag{2.29}$$

$$C_{v\psi} \frac{\mathrm{d}^3 v}{\mathrm{d}x^3} - C_{\psi\psi} \frac{\mathrm{d}^2 \psi_f}{\mathrm{d}x^2} + C_{\psi} \frac{\psi_f(x)}{h^2} = 0, \tag{2.30}$$

where dimensionless coefficients:

$$\overline{J}_z = \frac{1}{12}\left[1 - (1-\beta_0)\,\chi_{mp}^3\right] + (1-\beta_0) \int\limits_{-\chi_{mp}/2}^{\chi_{mp}/2} \eta^2 \sin^n\left(3\pi \frac{\eta}{\chi_{mp}}\right) \mathrm{d}\eta,$$

$$C_{v\psi} = 2\left\{ \int\limits_{\chi_{mp}/2}^{1/2} \eta\, f_d^{(lf)}(\eta)\,\mathrm{d}\eta + \int\limits_{0}^{\chi_{mp}/2} \eta\, f_d^{(mp)}(\eta)\; \overline{w}_{mp}(\eta)\,\mathrm{d}\eta \right\},$$

$$C_{\psi\psi} = 2\left\{ \int\limits_{\chi_{mp}/2}^{1/2} \left[f_d^{(lf)}(\eta)\right]^2 \mathrm{d}\eta + \int\limits_{0}^{\chi_{mp}/2} \left[f_d^{(mp)}(\eta)\right]^2 \overline{w}_{mp}(\eta)\,\mathrm{d}\eta \right\},$$

$$C_{\psi} = \frac{1}{1+\nu}\left\{ \int\limits_{\chi_{mp}/2}^{1/2} \left(\frac{\mathrm{d} f_d^{(lf)}}{\mathrm{d}\eta}\right)^2 \mathrm{d}\eta + \int\limits_{0}^{\chi_{mp}/2} \left(\frac{\mathrm{d} f_d^{(mp)}}{\mathrm{d}\eta}\right)^2 \overline{w}_{mp}(\eta)\,\mathrm{d}\eta \right\}.$$

The buckled shape of this beam is shown in Fig. 7.

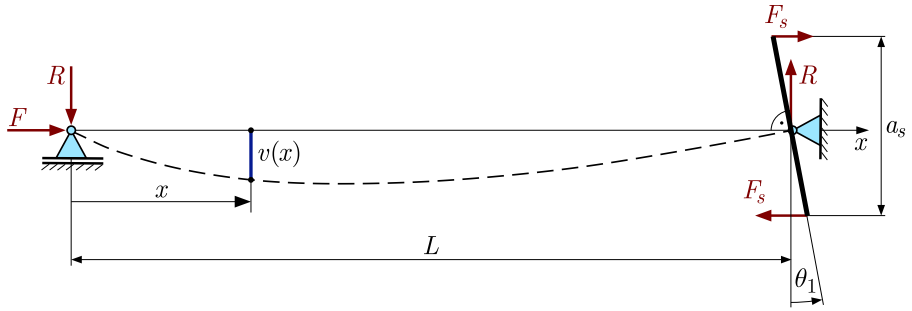

Fig. 7. Schematic diagram of the buckled shape of this beam.

The bending moment according to this diagram takes the following form:

$$M_b(x) = \left[-\overline{R}x + \overline{F}v(x)\right] Ebh, \tag{2.31}$$

where $\overline{R} = R/Ebh$, $\overline{F} = F/Ebh$ – dimensionless reaction and axial force.

Thus, the two differential equations of equilibrium (2.29) and (2.30) in the dimensionless coordinate, with consideration of expression (2.31), are as follows:

$$\overline{J}_z \frac{\mathrm{d}^2 v}{\mathrm{d}\xi^2} - C_{v\psi} L \frac{\mathrm{d}\psi_f}{\mathrm{d}\xi} + \lambda^2 \overline{F} v(\xi) = \xi \lambda^2 L \overline{R}, \tag{2.32}$$

$$C_{v\psi} \frac{\mathrm{d}^3 v}{\mathrm{d}\xi^3} - C_{\psi\psi} L \frac{\mathrm{d}^2 \psi_f}{\mathrm{d}\xi^2} + C_{\psi} \lambda^2 L \psi_f(\xi) = 0. \tag{2.33}$$

These two equations, after simple transformations, are reduced to one in the following form:

$$\frac{\mathrm{d}^4 v}{\mathrm{d}\xi^4} - k_2 \frac{\mathrm{d}^2 v}{\mathrm{d}\xi^2} - k_0 v(\xi) = -\xi\, \alpha^2 \frac{\lambda^4}{\overline{J}_z} \overline{R} L, \tag{2.34}$$

where $k_0 = \alpha^2 \frac{\lambda^4}{\overline{J}_z} \overline{F}$, $k_2 = \alpha^2 \lambda^2 \left(1 - \frac{C_{\psi\psi}}{\overline{J}_z C_{\psi}} \overline{F}\right)$, $\alpha = \sqrt{\frac{\overline{J}_z C_{\psi}}{\overline{J}_z C_{\psi\psi} - C_{v\psi}^2}}$ – dimensionless coefficients.

The solution of Eq. (2.34), with consideration of the boundary conditions, $v(0) = v(1) = 0$, is in the following form:

$$v(\xi) = \left[\xi - \frac{\sin(q\xi)}{\sin(q)}\right] \frac{\overline{R}}{\overline{F}} L, \tag{2.35}$$

where $q = \frac{1}{\sqrt{2}} \sqrt{-k_2 + \sqrt{k_2^2 + 4k_0}}$ – the dimensionless coefficient.

This function (2.35) describes the buckling line of the beam. Thus, the derivative of this function is given by

$$\frac{\mathrm{d}v}{\mathrm{d}\xi} = \left[1 - q \frac{\cos(q\xi)}{\sin(q)}\right] \frac{\overline{R}}{\overline{F}} L. \tag{2.36}$$

Consequently, the angle of rotation of the simply supported end of this beam ($\xi = 1$) with rotation limitation takes the following form:

$$\theta_1 = \left.\frac{\mathrm{d}v}{L\,\mathrm{d}\xi}\right|_1 = \left[1 - \frac{q}{\tan(q)}\right] \frac{\overline{R}}{\overline{F}}. \tag{2.37}$$

Based on Fig. 1 and Fig. 7, two expressions are formulated: $F_s a_s = RL$ and $F_s = \frac{1}{2}\theta_1 k_s a_s$, from which the angle rotation

$$\theta_1 = k_{\theta 1} \overline{R}, \tag{2.38}$$

where $k_{\theta 1} = \frac{2EbhL}{k_s a_s^2}$ – dimensionless coefficient, k_s – spring stiffness [N/mm], a_s – size [mm].

Equating both expressions (2.37) and (2.38), one obtains the algebraic equation

$$1 - \frac{q}{\tan(q)} + k_{\theta 1} \overline{F} = 0. \tag{2.39}$$

Based on this equation, the dimensionless critical force $\overline{F}_{CR}$ of this beam is determined.

Analyzing this equation, it is easy to notice two classic cases of support:

1) a simply supported beam for $k_s = 0$, $k_{\theta 1} \to \infty$, then $\tan(q) = 0$, from which $q = \pi$,
2) one clamped end for $k_s \to \infty$, $k_{\theta 1} = 0$, then $\tan(q) = q$, from which $q \cong 4.4934$.

Example calculations are carried out for the following data: $\chi_{mp} = 4/5$, $\beta_0 = 1/10$, $n = 10$, $\nu = 0.3$, $\lambda = 40$, and the dimensionless coefficient ($0 \le k_{\theta 1} < \infty$). The results of analytical calculations of the selected values of the dimensionless critical force $\overline{F}_{CR}$ are specified in Table 1.

Table 1. Values of the dimensionless critical force $\overline{F}_{CR}$ for the compressed beam.

$k_{\theta 1}$	0	2000	4000	7000	15000	30000	∞
$10^4 \overline{F}_{CR}$	6.93366	6.14493	5.60592	5.08517	4.42156	3.98617	3.41070

Moreover, these critical force values are graphically presented in Fig. 8.

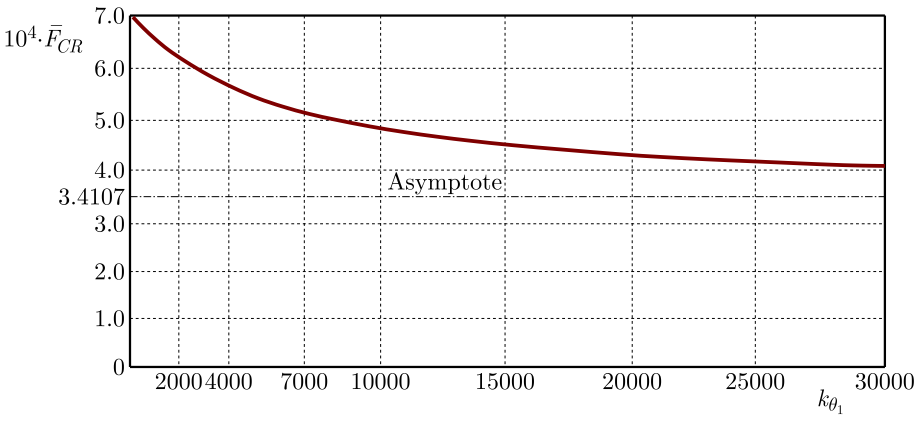

Fig. 8. Graph of the dimensionless critical force.

3. Analytical study of the individual I-beam without the shear effect

The two differential equilibrium Eqs. (2.32) and (2.33), in this case, are reduced to one in the following form:

$$\frac{\mathrm{d}^2 v}{\mathrm{d}\xi^2} + \frac{\overline{F}}{\overline{J}_z}\lambda^2 v(\xi) = \xi \frac{\overline{R}}{\overline{J}_z}\lambda^2 L. \tag{3.1}$$

The solution of Eq. (3.1), with consideration of the boundary conditions, $v(0) = v(1) = 0$, is in the following form:

$$v(\xi) = \left[\xi - \frac{\sin(k_F \xi)}{\sin(k_F)}\right] \frac{\overline{R}}{\overline{F}} L, \tag{3.2}$$

where $k_F = \sqrt{\overline{F}/\overline{J}_z}\lambda$ – dimensionless coefficient.

The derivative of this function is given by:

$$\frac{\mathrm{d}v}{\mathrm{d}\xi} = \left[1 - k_F \frac{\cos(k_F \xi)}{\sin(k_F)}\right] \frac{\overline{R}}{\overline{F}} L. \tag{3.3}$$

Consequently, the angle of rotation of the simply supported end of this beam ($\xi = 1$), with rotation limitation, takes the following form:

$$\theta_1 = \left.\frac{\mathrm{d}v}{L\,\mathrm{d}\xi}\right|_1 = \left[1 - \frac{k_F}{\tan(k_F)}\right] \frac{\overline{R}}{\overline{F}}. \tag{3.4}$$

This angle of rotation is consistent with the angle (2.38); therefore, by equating these two angles, one obtains the algebraic equation:

$$1 - \frac{k_F}{\tan(k_F)} + k_{\theta 1}\overline{F} = 0. \tag{3.5}$$

Based on this equation, the dimensionless critical force $\overline{F}_{CR}^{(0)}$ of this beam without the shear effect is determined. Similarly to the beam that considers the shear effect, when analyzing Eq. (3.5) for the two classic support cases, one obtains:

1) simply supported beam for $k_s = 0$, $k_{\theta 1} \to \infty$, then $\tan(k_F) = 0$, from which $k_F = \pi$, and so $\overline{F}_{CR}^{(0)} = \frac{\pi^2 \overline{J}_z}{\lambda^2}$,

2) one clamped end for $k_s \to \infty$, $k_{\theta 1} = 0$, then $\tan(k_F) = k_F$, from which $k_F \cong 4.4934$, and so $\overline{F}_{CR}^{(0)} = \frac{\pi^2 \overline{J}_z}{(0.699\lambda)^2}$.

Example calculations are carried out for the same data as for the beam with the shear effect. The results of the analytical calculations of the selected values of the dimensionless critical force $\overline{F}_{CR}^{(0)}$ are specified in Table 2.

Table 2. Values of the dimensionless critical force $\overline{F}_{CR}^{(0)}$ for the compressed beam.

$k_{\theta 1}$	0	2000	4000	7000	15000	30000	∞
$10^4 \overline{F}_{CR}^{(0)}$	7.01980	6.20522	5.65306	5.12268	4.45039	4.01093	3.43141

Taking into account the dimensionless critical force $\overline{F}_{CR}$ for the beam with the shear effect and the dimensionless critical force $\overline{F}_{CR}^{(0)}$ for the beam without the shear effect, the dimensionless shear effect coefficient of this beam is formulated as follows:

$$C_{SE} = 1 - \frac{\overline{F}_{CR}}{\overline{F}_{CR}^{(0)}}. \tag{3.6}$$

The example values of this coefficient are specified in Table 3.

Table 3. Values of the dimensionless shear effect coefficient C_{SE} for the beam.

$k_{\theta 1}$	0	2000	4000	7000	15000	30000	∞
$10^3 C_{SE}$	12.2710	9.7160	8.3388	7.3223	6.4781	6.1731	6.0354

Moreover, these dimensionless coefficient values of the shear effect are graphically presented in Fig. 9.

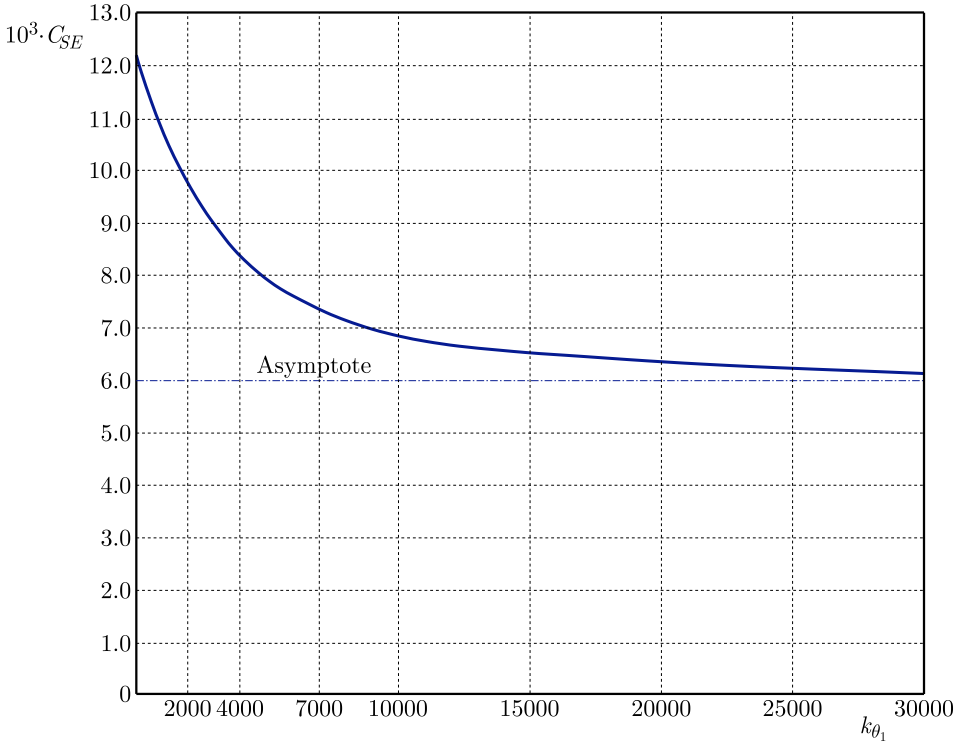

Fig. 9. Graph of the dimensionless coefficient of the shear effect.

The value of this dimensionless coefficient C_{SE} is small, so the influence of the shear effect on the critical force is insignificant.

4. Conclusions

The presented analytical studies of the elastic buckling problem for the individual I-beam, simply supported at the first end and with limited rotation at the second end, allow the following conclusions to be formulated:

- the applied procedure for analytically determining the deformation function of a planar beam cross-section is easy and effective (expressions (2.4)–(2.13)), (Figs. 3–5),
- the two different supports adopted at the beam ends make it possible to carry out tests on beams ranging from simply supported to clamped at one end (Table 1 and Fig. 8),
- the influence of the shear effect on the critical force values for the tested beam family is insignificant (Table 3 and Fig. 9).

References

1. Couto, C., Real, P.V., & Lopes, N. (2025). Local-global buckling interaction in steel I-beams—A European design proposal for the case of fire, *Thin–Walled Structures*, *206*, Part A, Article 112664. https://doi.org/10.1016/j.tws.2024.112664
2. Eslami, M.R. (2018). *Buckling and postbuckling of beams, plates, and shells*. Springer.
3. Filho, J.O.F., Tankova, T., Carvalho, H., Martins, C., & da Silva, L.S. (2022). Experimental and numerical flexural buckling resistance of high strength steel columns and beam-columns. *Engineering Structures*, *265*, Article 114414. https://doi.org/10.1016/j.engstruct.2022.114414
4. Genovese, D., & Elishakoff, I. (2019). Shear deformable rod theories and fundamental principles of mechanics. *Archive of Applied Mechanics*, *89*, 1995–2003. https://doi.org/10.1007/s00419-019-01556-7
5. Jing, J., Shao, Z.-H., Mao, X.-Y., Ding, H., & Chen, L.-Q. (2024). Forced resonance of a buckled beam flexibly restrained at the inner point. *Engineering Structures*, *303*, Article 117444. https://doi.org/10.1016/j.engstruct.2024.117444
6. Magnucki, K. (2024a). Bending of a five-layered composite beam with consideration of two analytical models. *Archive of Mechanical Engineering*, *71*(1), 27–46. https://doi.org/10.24425/ame.2024.149188
7. Magnucki, K. (2024b). Free flexural vibrations of standard wide-flange H-beams with consideration of the shear effect. *Rail Vehicles/Pojazdy Szynowe*, *1–2*, 46–50. https://doi.org/10.53502/RAIL-189244
8. Magnucki, K., & Milecki, S. (2015). Elastic buckling of a triangular frame subject to in-plane tension. *Journal of Theoretical and Applied Mechanics*, *53*(3), 581–591. http://doi.org/10.15632/jtam-pl.53.3.581
9. Magnucki, K., & Sowiński, K. (2024). Bending of a sandwich beam with an individual functionally graded core. *Journal of Theoretical and Applied Mechanics*, *62*(1), 3–17. https://doi.org/10.15632/jtam-pl/174698
10. Rykaluk, K. (2012). *Stability problems of metal constructions* (in Polish), Dolnośląskie Wydawnictwo Edukacyjne, Wrocław.
11. Simão, P.D. (2017). Influence of shear deformations on the buckling of columns using the Generalized Beam Theory and energy principles. *European Journal of Mechanics – A/Solids*, *61*, 216–234. https://doi.org/10.1016/j.euromechsol.2016.09.015
12. Szymczak, C., & Kujawa, M. (2019). Flexural buckling and post-buckling of columns made of aluminium alloy. *European Journal of Mechanics – A/Solids*, *73*, 420–429. https://doi.org/10.1016/j.euromechsol.2018.10.006
13. Yang, B., Zhang, Y., Xiong, G., Elchalakani, M., & Kang, S.-B. (2019). Global buckling investigation on laterally-unrestrained Q460GJ steel beams under three-point bending. *Engineering Structures*, *181*, 271–280. https://doi.org/10.1016/j.engstruct.2018.12.028
14. Yang, Y., Hui, Y., Li, P., Yang, J., Huang, Q., Giunta, G., Belouettar, S., & Hu, H. (2023). Global/local buckling analysis of thin-walled I-section beams via hierarchical one-dimensional finite elements. *Engineering Structures*, *280*, Article 115705. https://doi.org/10.1016/j.engstruct.2023.115705

Manuscript received March 13, 2025; accepted for publication May 13, 2025; published online September 4, 2025.